

Forecasting database for the tsunami warning center for the western Mediterranean Sea

Audrey Gailler, H el ene H ebert, Anne Loevenbruck, and Bruno Hernandez
CEA, DAM, DIF

F-91297, Arpajon, France
Audrey.gailler@cea.fr

Abstract—A first generation model-based tsunami prediction system is being developed as part of the French Tsunami Warning Center that will be operational by mid 2012. It involves a pre-computed unit source functions database (i.e., a number of tsunami model runs that are calculated ahead of time and stored) corresponding to tsunami scenarios generated by a source of seismic moment $1.75E+19$ N.m. In addition, an automated composite scenarios calculation tool is implemented to allow the simulation of any tsunami propagation scenario (i.e., of any seismic moment). The strategy is based on linear combinations and scaling of a finite number of pre-computed unit source functions. This tool produces maps with uncertainties (in epicenter location and magnitude) of expected maximum wave amplitude in deep ocean at each grid node rapidly. A no-dimension code representation is chosen to show zones in the main axis of energy at the basin scale. An example on the 2003 Boumerd es earthquake ($M_w=6.9$, northeastern Algerian margin) is presented. This forecast system provides warning refinement compared to the rough tsunami risk map given by the decision matrix.

Key words: tsunami, early warning system, forecasting database, Mediterranean sea

I. INTRODUCTION

Improvements in the availability of sea-level observations and advances in numerical modeling techniques are increasing the potential for tsunami warnings to be based on numerical model forecasts. Numerical tsunami propagation and inundation models are well developed, but they present a challenge to run in real-time, partly due to computational limitations and also to a lack of detailed knowledge on the earthquake rupture parameters.

In the frame of the French Tsunami Warning Center (FTWC) that will be operational by mid 2012, these numerical methods are adapted to contribute to future operational tools in charge to provide especially a map with uncertainties showing zones in the main axis of energy at the Mediterranean scale (i.e., deep ocean) rapidly. For this purpose, a strategy based on a pre-computed tsunami unit source functions database is developed, as source parameters available a short time after an earthquake occurs are preliminary and may be somewhat inaccurate. Existing numerical models are good enough to provide a useful guidance for warning structures to be quickly

disseminated. When an event will occur, an appropriate variety of offshore tsunami propagation composite scenarios by combining pre-computed propagation solutions (single or multi sources) may be recalled through an automatic interface (the pre-computed propagation solutions being stored as a unit source functions database). This approach will provide quick estimates of tsunami offshore propagation, and aid hazard assessment and evacuation decision-making.

As numerical model accuracy is inherently limited by errors in bathymetry and topography, and as inundation maps calculation is more complex and expensive in term of computational time, only tsunami offshore propagation modeling are included in the forecasting database. Far-field solutions are less sensitive to spatio-temporal details of the source (they depend primarily on the magnitude and location of the epicenter), and allow using a single sparse bathymetric computation grid for the numerical modeling. Moreover, working with deep ocean propagation modeling only enables to apply the properties of the linearity of the physics of tsunami generation and propagation in the ocean.

But a database of pre-computed results cannot contain all possible tsunami events, because of too much variability in the mechanism of tsunamigenic earthquakes. In principle, an infinite number of tsunami propagation scenarios can be constructed by linear combinations of a finite number of pre-computed “basis” scenarios. So a conservative approach is chosen, selecting the scenario –or interpolation between several scenarios- with the higher impact. The whole notion of a pre-computed forecasting database also requires a historical earthquake and tsunami database, as well as an up-to-date seismotectonic database including faults geometry and a zonation based on seismotectonic synthesis of source zones and tsunamigenic faults.

II. TSUNAMI RISK IN THE WESTERN MEDITERRANEAN SEA

The western Mediterranean Sea has been historically impacted by tsunamis triggered by earthquakes (Figure 1). However the generated waves were more moderate, and/or less documented than the ones usually reported in the eastern Mediterranean Sea (great tsunamis in Crete in 365 AD and 1305 AD).

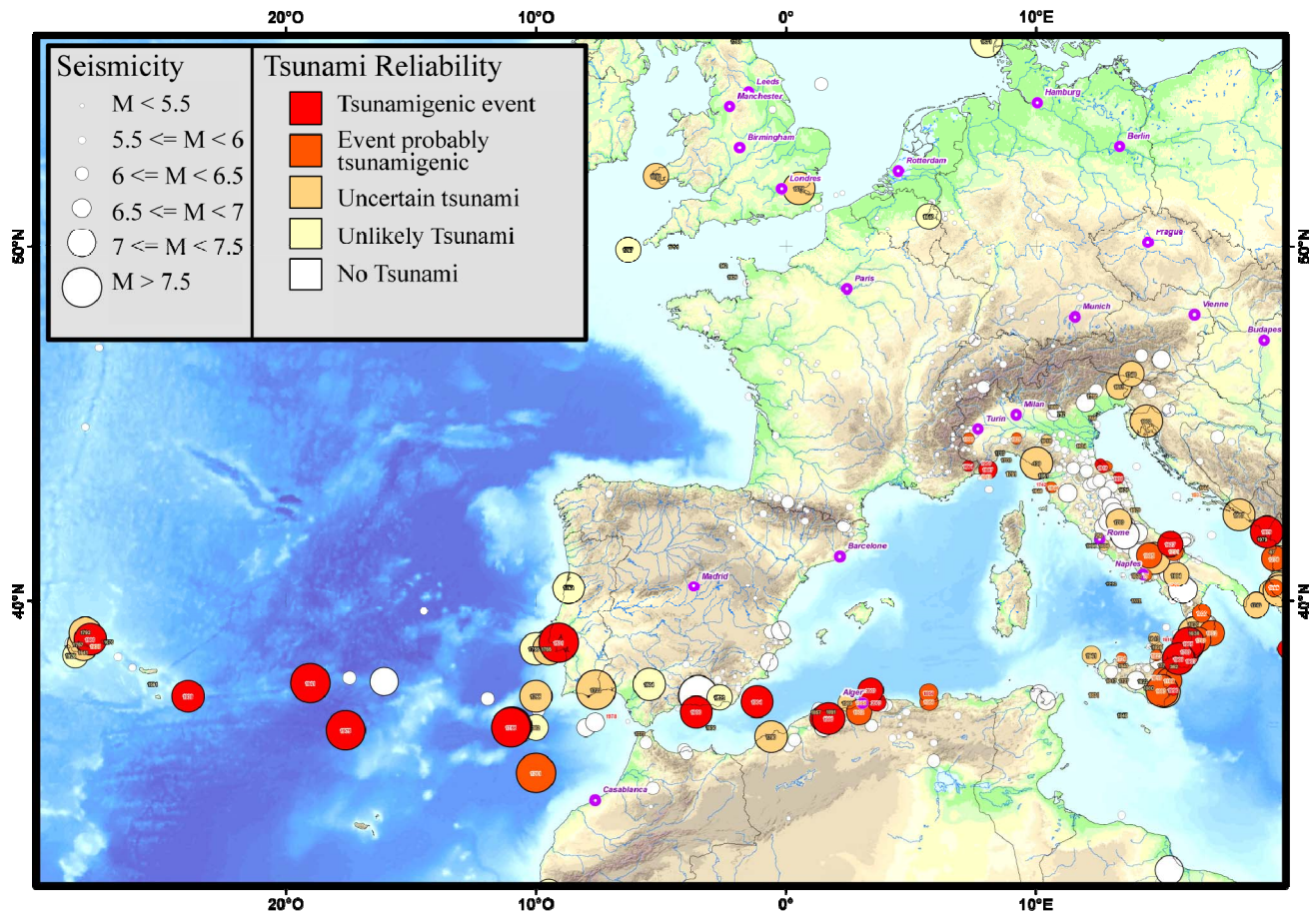


Figure 1. Historical tsunamigenic seismicity in western Mediterranean and north-east Atlantic.

In 1887, a strong earthquake in the Genoa Gulf, off Imperia (Italy) (magnitude 6.2 to 6.5), triggered an important tsunami that caused several floodings along the French Riviera, from Antibes to Menton. In Italy the 1908 earthquake and tsunami in the Messina straits caused more than 50000 casualties and nowadays offer a historical reference in South Italy. The North Algerian seismically active margin hosts several possibilities of strong submarine earthquakes able to produce important tsunamis in the western Mediterranean Sea, and the key recent event that recalled earthquake-induced tsunami awareness in the area occurred in May 2003, after the Boumerdès-Zemmouri earthquake (magnitude 6.9) in Algeria, which caused great damage and about 2000 casualties in the epicentral region.

The 2003 earthquake fault, even though characterized by a moderate magnitude as far as tsunami triggering is concerned (the tsunami threshold is close to magnitude 6.3 to 6.5), was however shallow and dip enough to produce a significant sea bottom deformation, which in turn triggered tsunami waves. In Algeria, the tsunami observations were very limited, either because steep submarine slopes do not favor amplification, or because the coastal areas were simultaneously uplifted due the coseismic deformation, thus preventing any inundation. But 30 min after the earthquake, the Balearic Islands were hit by significant tsunami waves which caused important damage in

several harbors, mostly on small pleasure crafts tied in various harbors in Majorca and Menorca. Limited inundations of peers or restaurant terraces have been very locally observed, for instance along the southeastern coastline of Majorca. Other quantitative observations were available through three good quality tide gauge records in Palma (Majorca), Sant Antoni and Menorca (Ibiza), which exhibited amplitudes from 0.5 (Palma) to 1.5 m (Sant Antoni) [1]. Elsewhere in the western Mediterranean, the amplitudes did not exceed 10 to 60 cm, but significant eddies, sea withdrawals were reported in several small pleasure harbors in southern France [2].

In the following, this Algerian event is chosen as test-case example to illustrate the composite scenarios calculation strategy developed and the resulting tsunami warning maps delivery in the frame of the FTWC.

III. COMPOSITE SCENARIOS CALCULATION STRATEGY

The calculation strategy is based on three main points:

- The implementation of a pre-computed unit source functions database
- The unit sources aggregation method chosen to obtain composite scenarios according to the magnitude of the detected earthquake
- The inclusion of uncertainties on the earthquake parameters

A. Pre-computed unit source functions database

The pre-computed unit source functions database is modeled on the western Mediterranean basin seismotectonic context. The latter being rather complex along the north Algerian margin especially, the choice has been made to draw a simplified fault base discretized in n unit sources and corresponding to the major structural trends of the area. Fault tracks on map (Figure 2) thus represent the top edge of the unit sources. Length (L) and Width (W) of each unit source are set at 25 km and 20 km respectively. Values of L and W are defined from empirical relations linking L and W to the magnitude M_w (Figure 3).

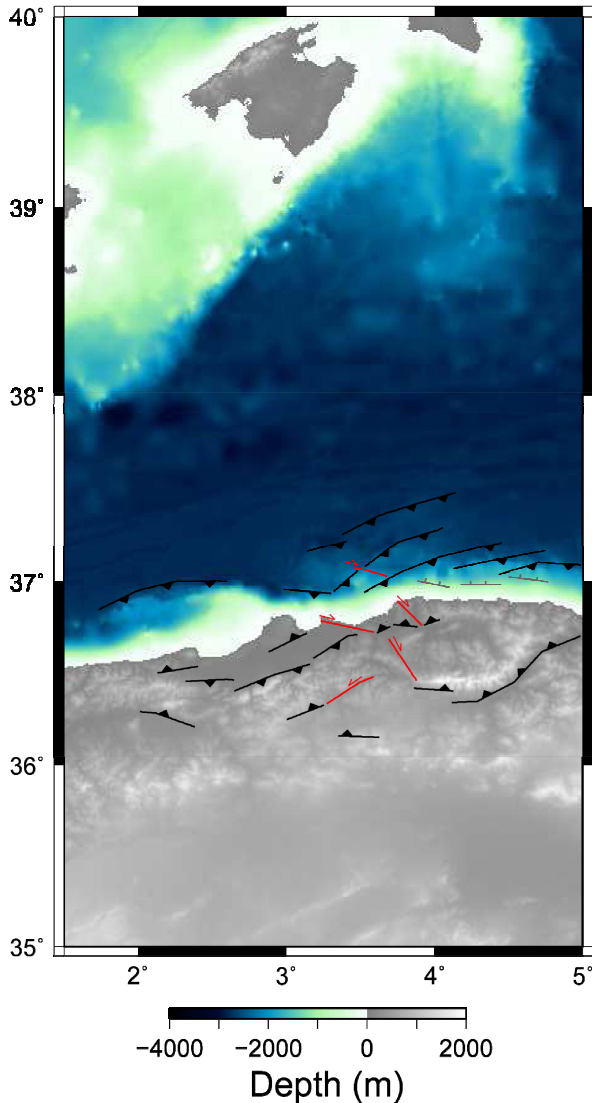


Figure 2. Simplified fault base used to create segments of 25 km length representing the top edge of each 25*20 km unit source function stored in the pre-computed database (detailed view on the Boumerdès area). (black) thrust faults; (grey) normal faults; (red) strike-slip faults.

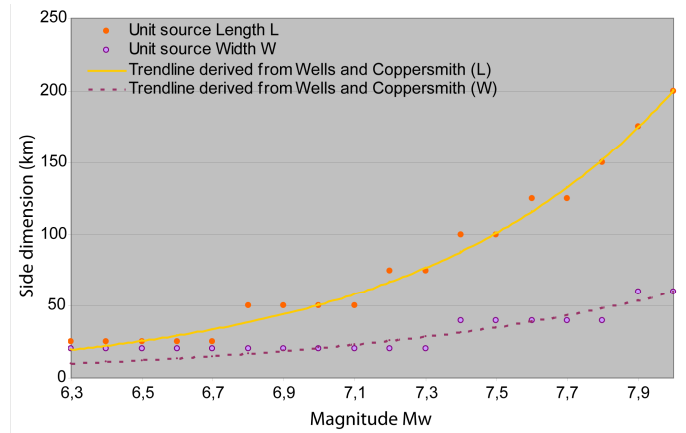


Figure 3. Comparison of the unit source length and width involved for a given magnitude as a function of the trendlines derived from [3] (i.e., equations (1) and (2)).

The corresponding equations are derived from [3], by fixing a length of 200km for a magnitude M_w of 8.0:

$$M_w = 4.135 + 1.679 \log_{10}(L) \quad (1)$$

$$M_w = 4.159 + 2.160 \log_{10}(W) \quad (2)$$

Figure 3 shows that the choice of 25*20 km² unit sources dimension correlates well with empirical trendlines (1) and (2), as the combination of an adequate number of close unit source functions enables to obtain, for each value of magnitude, rupture zone sizes compatible with these relations (e.g., 2 close unit sources giving a 50*25 km rupture area size for $M_w=7.0$, Figure 3).

For each unit source, a propagation scenario (wave heights) is calculated on a 2 minutes bathymetry grid (i.e., deep ocean modeling only), using the following other rupture zone parameters:

- 1 m slip (unitary)

- dip and rake regionalized based on the local seismotectonic history (keeping the most conservative values). The azimuth is given by the track of the fault on surface (i.e., top edge of rupture zone).

The numerical method used to simulate tsunami propagation from each unit source first allows the computation of the initial seafloor perturbation responsible for the tsunami triggering. In this framework, it consists of the static elastic dislocation accounting for the coseismic deformation. Then the propagation in the deep ocean is solved through a finite difference scheme taking into account the non linear terms of the depth-averaged hydrodynamical equations, hence under the non dispersive shallow water assumption (wave celerity c being simply given by $c = \sqrt{gh}$ where h is the water depth at each grid point) (see [4] for more details on the numerical method).

Each unit source function thus pre-computed and stored in base represents a tsunami generated by a fictive event of

magnitude $M_w=6.76$ ($M_0=1.75E+19$ N.m) with a rectangular rupture zone 25 by 20 km in size and 1 m in slip. From the north-east Algerian margin towards Messina Strait (Sicily), 500 such unit source functions compose the pre-computed propagation solutions database.

B. Composite scenarios calculation

As evoked in the previous paragraph, the number of unit source functions involved in a composite scenario calculation varies with the magnitude of the wanted solution (Figure 3, Table 1). Each composite scenario thus corresponds to a linear combination of x close unit source functions ($x=1$ to $2*8$), the resulting combined wave heights being multiplied by an appropriate scaling factor F_s . F_s is defined as a function of the magnitude M_w , exploiting the linearity of the physics of tsunami generation and propagation in the ocean. F_s calculation strategy is inspired from [5] who provide an enhanced tsunami forecasting database for the Joint Australian Tsunami Warning Center.

Considering the expression of the seismic moment M_0 as a function of earthquake rupture characteristics, i.e. $M_0=RWLu_0$ (with R shear modulus and u_0 slip of the rupture), any composite wave heights H_{comp} from an event with seismic moment $M_{0(comp)}=F_sM_0$ can be generated with the same rupture Length and Width but with a modified slip $u_{0(comp)}=F_su_0$. From the linearity of the physics of tsunami generation and propagation in the ocean, we can further assume than the wave heights from an event generated with a slip of F_su_0 are F_s times the wave heights H of an event with identical L and W , but a slip of u_0 :

$$H_{comp} = F_s H \quad (3)$$

Then the appropriate value for F_s is derived from the relation between magnitude M_w and seismic moment M_0 [$M_w=2/3(\log_{10} M_0-9.1)$]:

$$F_s = 10^{3/2(M_w(comp)-M_w)} \quad (4)$$

A summary of the scaling factors thus determined for our forecasting database is provided in Table 1 (calculation done with $R=35E+9$ N/m²). In each case, the new composite scenario is scaled from one or the combination of several unit source functions following the best fits between rupture dimensions (L and W) and the wanted magnitude $M_w(comp)$ (i.e., equations (1) and (2)). For example, in the case of the 2003 Boumerdès earthquake for which the magnitude was estimated at $M_w=6.9$, the representative composite scenarios are obtained from either a single unit source function scaled by 1.61, or the linear combination of two close unit source functions multiplied by a factor of 0.81. In order to be as conservative as possible, the composite scenario calculations take also into account the inaccuracy on the epicenter location of the detected event (for instance set at a 30 km search radius) and the uncertainty on the associated estimated magnitude. The latter is set at ± 0.2 but this value will depend on the seismic network azimuthal coverage that will be operational in 2012.

TABLE 1. SCALING FACTORS (F_s) REQUIRED TO PRODUCE A COMPOSITE SCENARIO OF MAGNITUDE $M_w(comp)$ FROM THE EXISTING $25*20$ KM² UNIT SOURCE FUNCTIONS.

$M_w(comp)$	Nb of unit sources involved (25*20 km)	Length L (km)	Width W (km)	Existing M_w	F_s
6.5	1	25	20	6.76	0.40
6.6	1	25	20	6.76	0.57
6.7	1	25	20	6.76	0.81
6.8	1	25	20	6.76	1.14
6.8	2	50	20	6.96	0.57
6.9	1	25	20	6.76	1.61
6.9	2	50	20	6.96	0.81
7.0	2	50	20	6.96	1.14
7.1	2	50	20	6.96	1.61
7.2	2	50	20	6.96	2.27
7.2	3	75	20	7.08	1.51
7.3	3	75	20	7.08	2.14
7.3	2*4	100	40	7.36	0.80
7.4	3	75	20	7.08	3.02
7.4	2*4	100	40	7.36	1.13
7.5	2*4	100	40	7.36	1.60
7.6	2*4	100	40	7.36	2.26
7.6	2*5	125	40	7.43	1.81
7.7	2*4	100	40	7.36	3.19
7.7	2*5	125	40	7.43	2.55
7.8	2*5	125	40	7.43	3.61
7.8	2*6	150	40	7.48	3.00
7.9	2*6	150	40	7.48	4.24
7.9	2*7	175	40	7.53	3.64
8.0	2*8	200	40	7.56	4.50

IV. FINAL COMPOSITE SCENARIO CONSTRUCTION: EXAMPLE ON THE M_w 6.9 2003 BOUMERDÈS EVENT

A. Inaccuracy on the epicenter location: composite solutions available within a 30 km search radius

As the inaccuracy on the epicenter must be taken into account, the following methodology has been chosen:

- (1) the first stage consists of searching automatically all the pre-computed unit sources localized within a circle whose center is the estimated epicenter of the detected event and whose radius is in this case set at 30 km (but configurable). Practically the distance between the epicenter and the middle of the top edge of each unit source is used.

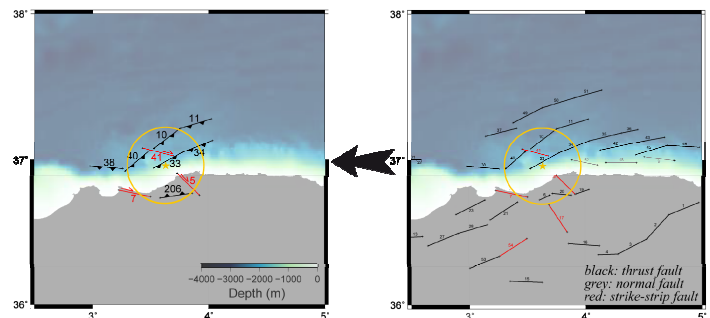


Figure 4. Detailed view on the 2003 Boumerdès earthquake and pre-computed unit source functions available in the area. (yellow star) epicenter of the event, (yellow circle) inaccuracy search radius.

In the case of the 2003 Boumerdès earthquake, 7 unit source functions stored in the pre-computed database are within the 30 km search radius (i.e., unit source functions number 40, 41, 10, 33, 5, 206 and 7 in Figure 4).

(2) Considering an estimated magnitude of $M_w=6.9$ for this event, 12 different possible solutions are then available following Table 1, i.e.:

- 7 solutions using a single unit source function with $F_s=1.61$ (unit source number written above)
- 5 solutions using a linear combination of 2 close unit sources with $F_s=0.81$ (i.e., combination of unit sources number 40+38, 40+10, 10+11, 33+34 and 33+40, Figures 4 and 5). The combination is done only on faults of the same type (thrust, normal or strike-slip) and with azimuthal and distance conditions.

Note that if no unit source is found within a maximum search radius (i.e., no a priori seismotectonic information known in the considered area), the process is aborted and only the map derived from the decision matrix will be produced (see section IV.C.).

B. Combination scheme of the maximum wave heights

Figure 5 illustrates the automated calculation process developed to obtain the final composite scenario from the pre-computed database, taking into account the inaccuracy on epicenter location (i.e., Boumerdès earthquake) for a given

magnitude (i.e., $M_w 6.9$). Maximum wave heights (H_{max}) are represented after 3 hours of propagation.

The automated calculation process can be divided in 3 steps:

- (1) search of the unit source functions stored in the pre-computed database within a 30 km radius from the epicenter of the event. Smallest contoured maps in Figure 5 represent the H_{max} for the 10 pre-computed unit source functions answering this criteria. Each of these propagation simulations corresponding to a fictive magnitude of $M_w=6.76$.
- (2) Composite solutions calculation as a function of the magnitude of the detected event and of the combination and scaling parameters of Table 1. Medium contoured maps show the 12 H_{max} composite solutions of $M_w=6.9$ resulting from the 10 pre-computed unit source functions identified in step 1, with conditions on the fault type and geometry as mentioned in section IV.A. (last point).
- (3) Final composite H_{max} calculation (large map on the left, Figure 5) as the maximum wave heights from the 12 solutions of step 2 at each grid node. This final composite scenario corresponds to the same $M_w=6.9$ event, including the inaccuracy on the epicenter location (being the most conservative).

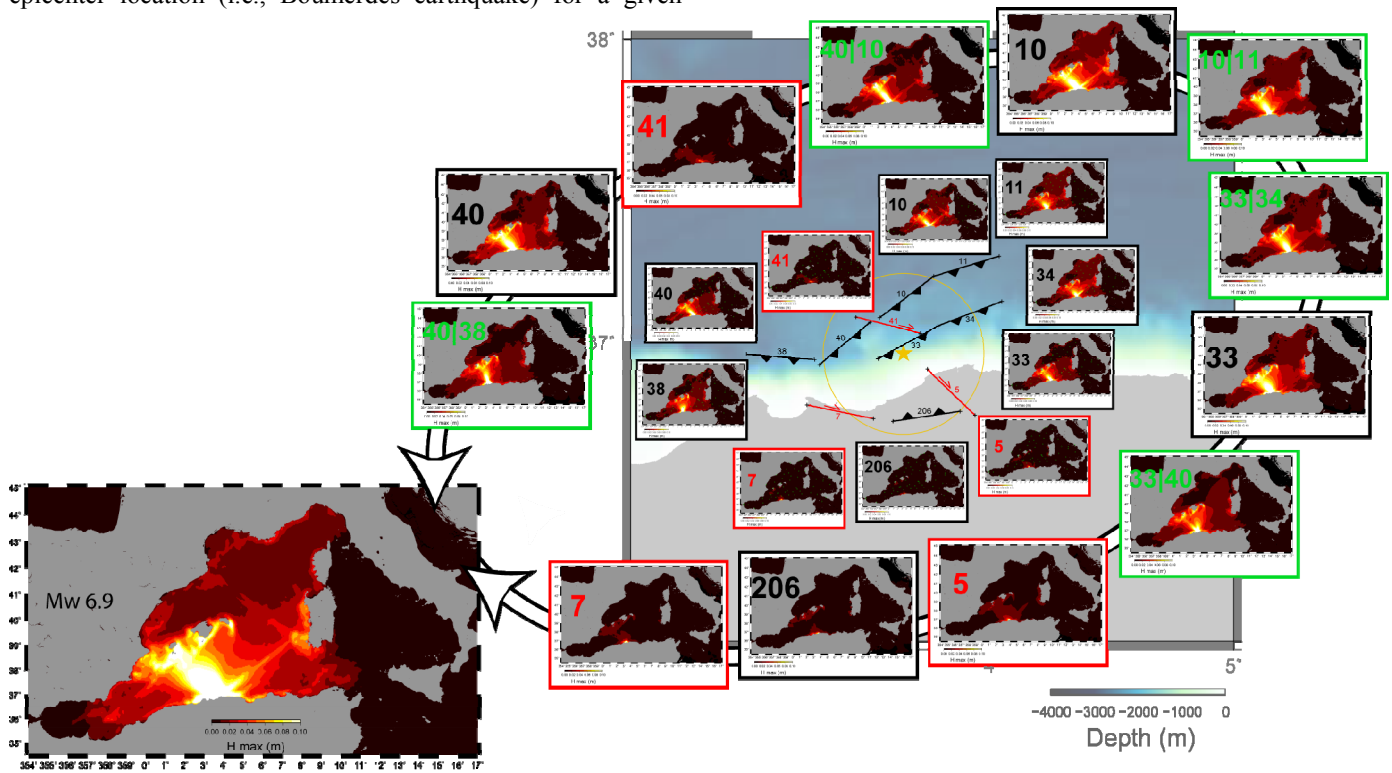


Figure 5. Composite scenarios calculation process using the test-case of the 2003 Boumerdès earthquake ($M_w 6.9$, Algeria). (Smallest maps) maximum wave heights stored as unit source functions ($M_w=6.76$) in the pre-computed database and involved in this case; (Medium maps) $M_w 6.9$ derived composite scenarios solutions form a single unit source (red contour for strike-slip source and black contour for thrust source) or the combination of two (green contour, thrust source only); (Large map, left) final composite solution for $M_w=6.9$ from all medium maps (including the inaccuracy on the epicenter location).

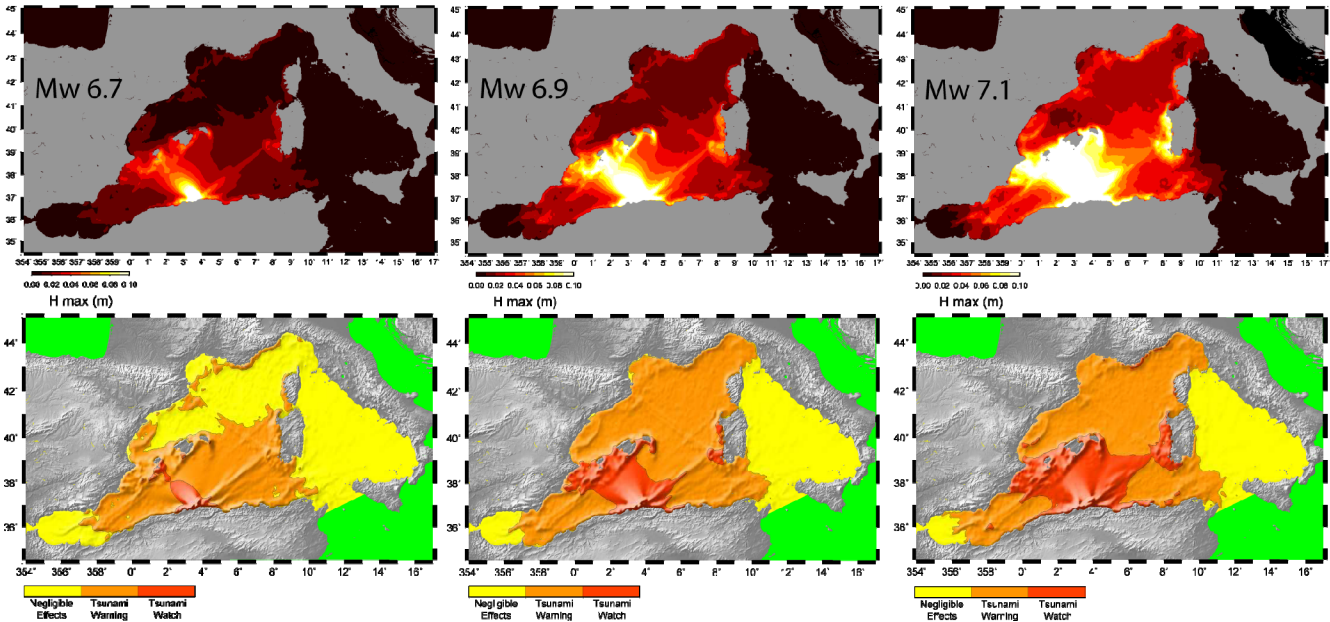


Figure 6. (top) Maximum wave heights obtained for the three final composite scenarios of the same event, taking into account the uncertainty on the magnitude (+/- 0.2); and (bottom) corresponding representation with a no-dimension tsunami warning code (after 3 hours of real time propagation).

C. Final composite solutions with uncertainty on the magnitude

As the source parameters available a short time after an earthquake occurs are preliminary and somewhat inaccurate, an uncertainty on the estimated magnitude of the detected event must be taken into account. Thus, it has been chosen to proceed, for Mw -0.2 and Mw +0.2, to the same calculation process as the one depicted in Figure 5 and section IV.B. That means, that for the same event, 3 final composite scenarios are produced (respectively representative of Mw, Mw-0.2 and Mw+0.2), each one including the inaccuracy on the epicenter location. For the 2003 Boumerdès earthquake, this implies the additional calculation for magnitudes Mw 6.7 and 7.1, with corresponding combination and scaling parameters of Table 1 (Figure 6).

The deep ocean maximum wave heights thus produced from the forecast system are then transposed in a no-dimension warning colors code by a simple normalization of the 3 Hmax provided by the corresponding final composite scenarios by a fixed factor (Figure 6). They can be interpreted as the most likely scenario and its minimal and maximal bounds, and express the tsunami warning in deep ocean, being as conservative as possible in term of source parameters. These no-dimension representations will be delivered to the authorities within 8 hours after the tsunamigenic event detection in the frame of the FTWC, together with the map given by the decision matrix (with the same no-dimension scale) (Figure 7).

The map obtained from the decision matrix is established from the detected event magnitude and the distance between coasts and the epicenter (Table 2). It offers a rough representation of the tsunami warning at the basin scale,

whether the 3 maps coming from the pre-computed unit source functions database add in refinement looking at the source directivity: the main axis of tsunami energy highlights clearly more focused warning sectors. In the case of the 2003 Boumerdès earthquake, the red zone of “tsunami watch” is defined by the decision matrix as a 400 km radius circle around the event epicenter. The most likely composite scenario shows a refinement of this red zone towards the Balearic coasts especially, and the western Sardinia coasts locally. In the frame of the FTWC, the forecasting system will be triggered automatically as soon as a potential tsunamigenic event will be detected.

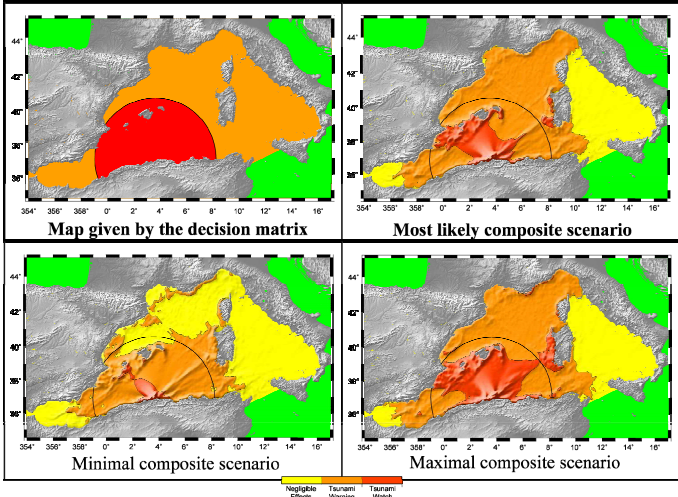


Figure 7. Final representation produced by the forecasting system to be delivered to the authorities 8 hours after the detection of a tsunamigenic earthquake. (black circle) 400 km radius warning area around the epicenter defined by the decision matrix; (green zones) area not included in the western Mediterranean basin.

TABLE 2. Decision matrix for the western Mediterranean basin.

Depth	Location	Mw	Tsunami Potential	Type of Bulletin
< 100 km	Offshore or close to the coast (≤ 40 km inland)	5.5 à 6.0	weak potential of local tsunami	Information Bulletin
		6.0 à 6.5	Potential of destructive local tsunami < 100 km	Regional Tsunami Advisory
		6.5 à 7.0	Potential of destructive regional tsunami < 400 km	Regional Tsunami Watch - Basin-wide Tsunami Advisory
	Offshore or close to the coast (≤ 100 km inland)	≥ 7.0	Potential of destructive tsunami in the whole basin > 400 km	Basin-wide Tsunami Advisory
	Inland (> 40 km and ≤ 100 km)	5.5 à 7.0	weak potential of local tsunami	Information Bulletin
≥ 100 km	Offshore or inland (≤ 100 km)	≥ 5.5	Nil	Information Bulletin

D. Comparison with “on the fly” tsunami modeling

As the forecasting system provides wave heights information at the basin scale only (i.e., does not take into account the coastal response to tsunami arrival), evaluations against tide gage observations are unsuitable. And there is currently no tsunamimeter in the Mediterranean sea. So the idea is to evaluate the forecasting system products through a comparison with a tsunami modeling in deep ocean using the same numerical method, but taking as source parameter a rupture geometry relying on more realistic seismotectonic patterns. The coseismic deformation of the 2003 Boumerdès earthquake has been widely studied (e.g., [6], [7], [8]), being among the largest events to occur in the western Mediterranean over the past 25 years. For the comparison, we choose to use the source parameters proposed by [8], whose characteristics are a reverse rectangular fault plane of 32 km length by 14 km width. The azimuth, dip, rake and slip values are N60°, 42°S, 84° and 1.8 m respectively. The epicenter depth is set at 8.7 km (i.e., rupture does not reach the surface).

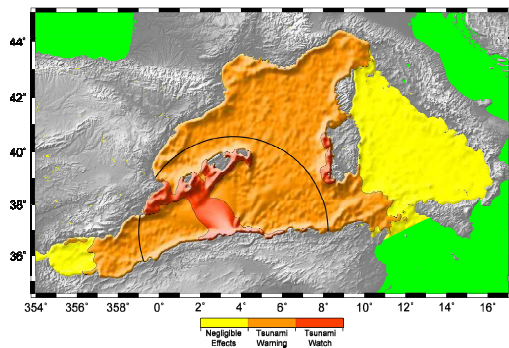


Figure 8. Warning map resulting from the “on the fly” tsunami modeling, using the source parameters of [8]. Color scale same as Figure 7.

Considering a shear modulus of $R=35E+9$ N/m², this source corresponds to an event of seismic moment $M_0=2.82E+19$ N.m (i.e., Mw=6.9). The numerical modeling is then run on the same 2 minutes bathymetry grid as the one used in the forecasting system, and the resulting computed maximum wave heights are transposed in the conventional no-dimension warning scale depicted previously (Figure 8).

The warning map obtained with this “on the fly” simulation is clearly consistent with the ones derived from the pre-computed unit source functions database (Figure 7). In term of risk assessment, it takes place between the ‘minimal composite scenario’ and the ‘most likely composite scenario’, but being closer to the latter. The same tsunami watch sectors (red zones) are highlighted, i.e. Balearic coasts and western Sardinia coasts locally. This evaluation shows that the forecasting system provides coherent tsunami warning information.

V. CONCLUSION

The forecast strategy chosen for the FTWC is based on a unit source function methodology, whereby the pre-modeled runs are combined and linearly scaled to produce any composite tsunamis propagation solution. Each unit source function is equivalent to a tsunami generated by a M_0 1.75E+19 N.m earthquake with a rectangular fault 25 km by 20 km in size and 1 m in slip. The faults of the unit functions are placed adjacent to each other, following the discretization of the main seismogenic faults bounding the western Mediterranean basin. The number of unit functions involved varies with the magnitude of the wanted composite solution and the combined wave heights are multiplied by a given scaling factor to produce the new arbitrary scenario. Uncertainty on the magnitude of the detected event and inaccuracy on the epicenter location are taken into account in the composite scenarios calculation. For one tsunamigenic event, 3 no-dimension scale warning maps are finally produced (i.e., most likely, minimum and maximum scenarios) together with the rough decision matrix representation.

ACKNOWLEDGMENT

We thank Alain Rabaute for his work on the seismotectonic synthesis of the western Mediterranean basin.

REFERENCES

- [1] P.J. Alasset, H. Hébert, V. Calbini, S. Maouche, and M. Meghraoui, "The tsunami induced by the 2003 Zemmouri earthquake (Mw=6.9, Algeria): modeling and results," *G.J.Int.*, 166, 213-226, 2006.
- [2] A. Sahal, J. Roger, S. Allgeyer, B. Lemaire, H. Hébert, F. Schindelé, and F. Lavigne, "The tsunami triggered by the 21 May 2003 Boumerdès-Zemmouri (Algeria) earthquake: field investigations on the French Mediterranean coast and tsunami modeling," *NHESS*, 9, 1823-1834, 2009.
- [3] D.L. Wells, and K.J. Coppersmith, "New empirical relationships among magnitude, rupture length, rupture width, rupture area, and surface displacement," *Bull. Seismol. Soc. Am.*, 84(4), 974-1002, 1994.
- [4] H. Hébert, D. Reymond, Y. Krien, J. Vergoz, F. Schindelé, J. Roger, and A. Loevenbruck, "The 1(August 2007 Peru earthquake and tsunami: influence of the source characteristics on the tsunami heights," *Pageoph*, 166, 1-22, 2009.
- [5] D.J.M. Greenslade, M.A. Simanjuntak, and C.R.A. Stewart, "An enhanced tsunami scenario database: T2, Centre for Australian Weather and Climate Research (CAWCR)," *CAWCR Technical Report*, 14, 2009.
- [6] F. Semmane, M. Campillo, and F. Cotton, "Fault location and source process of the Boumerdès, Algeria, earthquake inferred from geodetic and strong motion data," *Geophys. Res. Lett.*, 32, 2005.
- [7] M. Meghraoui, S. Maouche, B. Chemaa, Z. Cakir, A. Aoudia, A. Harbi, P.J. Alasset, A. Ayadi, Y. Bouhadad, and F. Benhamouda, "Coastal uplift and thrust faulting associated with the Mw=6.8 Zemmouri (Algeria) earthquake of 21 May, 2003," *Geophys. Res. Lett.*, 31, 2004.
- [8] K. Yelles, K. Lammali, A. Mahsas, E. Calais, and P. Briole, "Coseismic deformation of the May 21st, 2003, Mw=6.8 Boumerdès earthquake, Algeria, from GPS measurements," *Geophys. Res. Lett.*, 31, 2004.